Vertical-Cavity Surface-Emitting Laser With Thermally Induced Birefringence

Tobias Pusch and Eros La Tona

Birefringent vertical-cavity surface-emitting lasers offer a new opportunity to generate high polarization modulation dynamics. By inducing spin-polarized carriers, the device can be excited to oscillations in the degree of circular polarization with an oscillation frequency nearly equal to the birefringence splitting. A mechanism for frequency tuning of the oscillations directly integrated on the chip is desirable for future applications. With asymmetric heating we demonstrate a reversible tuning of the birefringence splitting of 45 GHz with a decrease of the laser output power of less than 3 dB.

1. Introduction

Vertical-cavity surface-emitting lasers (VCSELs) are used extensively today for optical sensing and data transmission [1]. While most sensing applications impose only very moderate requirements on the device dynamics, VCSELs in data transmission systems are optimized for high bandwidth. Digital data transmission at a data rate of 50 Gb/s using a bit pattern generator [2] and at 71 Gb/s with a dedicated electronic driver chip employing transmitter equalization [3] have been published. Recently as much as 150 Gb/s were generated with a commercial 850 nm wavelength VCSEL with 23 GHz bandwidth that was modulated with a spectrally efficient 13-level signal (modified duobinary 4-level pulse amplitude modulation). Offline digital signal processing was required to determine bit error ratios [4]. To reduce the system complexity and increase the energy efficiency, laser devices with substantially higher bandwidth are needed for future optical interconnects with data rates exceeding 100 Gb/s. The polarization dynamics in VCSELs offers benefits to overcome the limitations of intensity modulation. Here the birefringence splitting, namely the frequency difference between the two linearly polarized modes, plays an important role. By injection of spin-polarized carriers into a birefringent VCSEL, an oscillation in the degree of circular polarization can be generated, while the average emitted power remains constant [5]. This oscillation can be switched off in an extremely short time interval [6]. Fast polarization oscillations based on induced spin were shown [7]. The oscillation frequency is nearly equal to the birefringence splitting. A measured birefringence splitting of more than 250 GHz shows the potential of this approach [8].

2. New VCSEL Concept for Asymmetric Heating

A high birefringence splitting in VCSELs can be obtained using the elasto-optic effect. External strain can induce a lattice anisotropy which results in an anisotropic change of

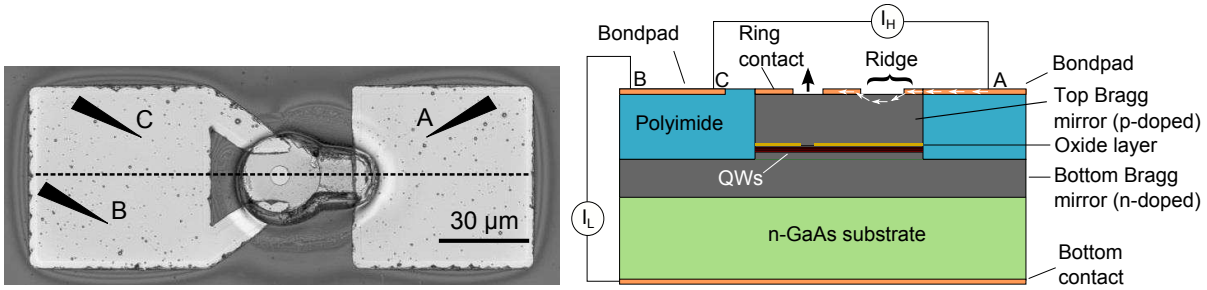

Fig. 1: Photograph of a fabricated device (left). Cross-section of the VCSEL structure along the dotted line on the left with the two electrical circuits (right). The path of the heating current is partly indicated with white arrows. A, B, and C mark the contact points of the probe needles.

the refractive index. With this approach Panajotov et al. [9] reported a birefringence splitting of 80 GHz in a VCSEL packaged in a TO-can. Direct mechanical bending of a VCSEL array has resulted in the present record of $B = 259$ GHz birefringence splitting [8]. For mechanically induced strain, a custom-made bending device is needed. This limits the miniaturization of the laser sub-system as well as later commercial applicability. Alternatively the birefringence splitting can be induced thermally. Jansen van Doorn et al. [10, 11] used a 770 nm Ti:sapphire laser to generate a hotspot approximately 30 µm next to the emission window of an 850 nm VCSEL. With a laser output power of 27 mW a reversible birefringence tuning of $B < 3$ GHz was measured [10] and a much higher power of 200 mW led to a change of the birefringence to $B = 23$ GHz accompanied by surface damage [11], which is unacceptable for practical use. After the heating power was shut off, a few percent of the birefringence change reached by exposure remained [11].

The approach reported in this article is based on the same idea of asymmetric heating. However, we replace the external optical power source by an integrated electrical heater. Such a one-chip device combines very small size, ease of handling, and fine-tuning capability of the birefringence splitting. A top view of the fabricated VCSEL structure and a schematic cross-section are shown in Fig. 1. Wafer material for standard oxide-confined AlGaAs-based 850 nm VCSELs was used, which was grown on a n-doped (001)-oriented GaAs substrate by Philips Technologie GmbH, U-L-M Photonics. It consists of a p-i-n structure with 23 top Bragg mirror pairs in the p-region and 37.5 bottom mirror pairs in the n-region. The inner one-wavelength-thick cavity has three GaAs quantum wells (QWs). An adjacent 30 nm thick AlGaAs layer in the p-region serves for current confinement after mesa etching and wet-thermal oxidation. In contrast to conventional VCSELs the mesa is not circular but resembles the shape of a keyhole. The orientation is along the [110] or [$\bar{1}$10] crystal axis, which are the preferred orthogonal polarization directions of standard GaAs VCSELs [1]. The etching with a depth of 4.8 µm extends well into the n-region. The VCSEL mesa has a diameter of 26 µm and the connected ridge has a length and width of 16 µm and 12 µm, respectively. The oxidation step produces a fully oxidized ridge and an aperture of 4–5 µm diameter for transverse single-mode emission of the laser. The top p-ring contact on the mesa made of TiPtAu has an opening of 8 µm. The bottom contact metalization is GeAuNiAu. The two bondpads in Fig. 1 are placed on polyimide which is necessary for electrical insulation and planarization. They are connected to the

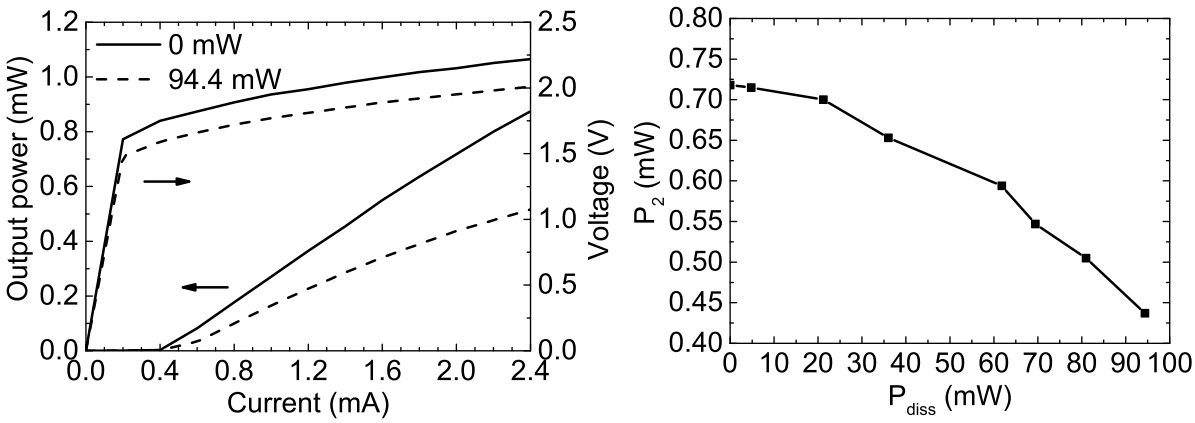

Fig. 2: LIV curves of the VCSEL at 0 mW and 94.4 mW heating power (left). Laser output power $P_2 = P(I_\mathrm{L} = 2\,\mathrm{mA})$ versus dissipated power $P_\mathrm{diss} = I_\mathrm{H} \cdot V_\mathrm{H}$ in the heater (right).

p-ring contact on one side and a short contact metalization (not covering the entire ridge, see Fig. 1(right)) at the edge of the ridge on the other side. Two electrical circuits provide a high heating current I_H and a low VCSEL operating current I_L simultaneously. As sketched in Fig. 1(right) the heating current flows from the right bondpad through the ridge to the VCSEL ring contact and the left bondpad. The metalization gap forces the current to enter the semiconductor ridge material with much reduced conductivity. This is where the majority of heat generation takes place. The positions of the contact needles are marked with A and C in Fig. 1. The fully oxidized ridge area is necessary to prevent current flow through the ridge to the bottom contact. The second current path through the VCSEL aperture to the bottom contact (contact point B) is used for laser operation.

3. Measurement Results

The measured light–current–voltage (LIV) characteristics for VCSEL operation without heating are shown in Fig. 2(left). The threshold current is $I_\mathrm{th} = 0.42\,\mathrm{mA}$ at a voltage of $V_\mathrm{th} = 1.76\,\mathrm{V}$. The slope efficiency is 0.46 W/A, corresponding to a differential quantum efficiency of 31 %. Figure 3 depicts the optical spectrum of the unheated VCSEL at a current of $I_\mathrm{L} = 2.3\,\mathrm{mA}$. It has two peaks at wavelengths of 848.00 nm and 848.04 nm. These are the orthogonal polarization states of the fundamental mode. Actually the spectrum was measured with a polarizer suppressing the longer-wavelength mode by about 28 dB. Otherwise, caused by the resolution of the optical spectrum analyzer of 0.015 nm, only this peak would be visible and the initial birefringence splitting couldn't be determined. The observed wavelength difference $\Delta\lambda = 0.04\,\mathrm{nm}$ of the polarization modes corresponds to a birefringence splitting $B = \Delta\nu = c\Delta\lambda/\lambda^2 = 17\,\mathrm{GHz}$, where c is the vacuum velocity of light. The next-order transverse mode at $\lambda \approx 847\,\mathrm{nm}$ is not seen in the spectrum. The side-mode suppression ratio of the VCSEL (without polarizer) is about 26 dB at the given operating point.

In what follows the device is characterized for different amounts of heating up to a current $I_\mathrm{H} = 33\,\mathrm{mA}$. This maximum value is chosen in order to prevent contact damage. Figure

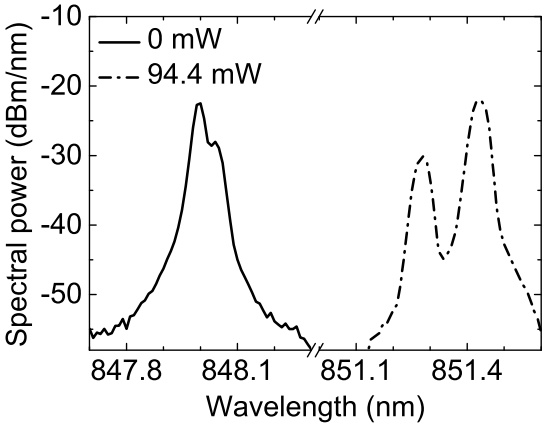

Fig. 3: Measured optical spectra without heating and for $P_{\mathrm{diss}} = 94.4\,\mathrm{mW}$. A polarizer has suppressed the long-wavelength peak at 848.04 nm and the short-wavelength peak at 851.28 nm. The laser current is $I_L = 2.3\,\mathrm{mA}$.

2(left) shows the LIV curves for the peak dissipated power $\hat{P}_{\mathrm{diss}} = \hat{I}_{\mathrm{H}} \cdot \hat{V}_{\mathrm{H}} = 33\,\mathrm{mA} \cdot 2.86\,\mathrm{V}$ $= 94.4\,\mathrm{mW}$. The purpose of heating is the creation of anisotropic strain in the laser cavity by means of the elasto-optic effect. While doing so, the laser necessarily experiences a parasitic temperature increase, which is known to decrease both the achievable output power and the operating voltage [1]. In the given device the slope efficiency decreases from $0.46\,\mathrm{W/A}$ at $I_{\mathrm{H}} = 0$ to $0.30\,\mathrm{W/A}$ at $I_{\mathrm{H}} = 33\,\mathrm{mA}$. The effect of the dissipated power P_{diss} on the output power at a laser current of $I_{\mathrm{L}} = 2\,\mathrm{mA}$ is displayed in Fig. 2(right). The decrease from initially $0.72\,\mathrm{mW}$ to $0.44\,\mathrm{mW}$ for maximum heating amounts to less than 40 % and is thus well acceptable. Most importantly the birefringence splitting of the fundamental mode in the optical spectrum in Fig. 3 has become much larger. The measured wavelength difference of $\Delta\lambda = 0.15\,\mathrm{nm}$ corresponds to $B = 62\,\mathrm{GHz}$ and thus the VCSEL can be tuned by as much as $\Delta B = (62-17)\,\mathrm{GHz} = 45\,\mathrm{GHz}$. The spectrum of the heated device in Fig. 3 was measured with the polarizer rotated by 90° versus the case $I_{\mathrm{H}} = 0$. Obviously now the short-wavelength polarization mode at $\lambda = 851.28\,\mathrm{nm}$ dominates. The underlying polarization switch was found to occur at $I_{\mathrm{H}} \approx 30\,\mathrm{mA}$. Figure 4 plots the birefringence splitting as a function of the dissipated power. There is a continuous increase of B with increasing P_{diss} with an apparent change of the slope around $P_{\mathrm{diss}} = 60\,\mathrm{mW}$, which is in the vicinity of the polarization switching point.

4. Conclusion

In summary we have presented a novel VCSEL device with electrical tunability of the birefringence splitting via asymmetric heating. A record-high thermally induced tuning range of 45 GHz was shown at a moderate reduction of the laser output power. Even higher values should be achievable with a more robust contact design allowing higher heating currents. Fully reversible behavior without a remanent birefringence change was observed. The detailed birefringence tuning behavior close to a polarization switching point is a topic for further studies. The integrated heating approach can be combined with

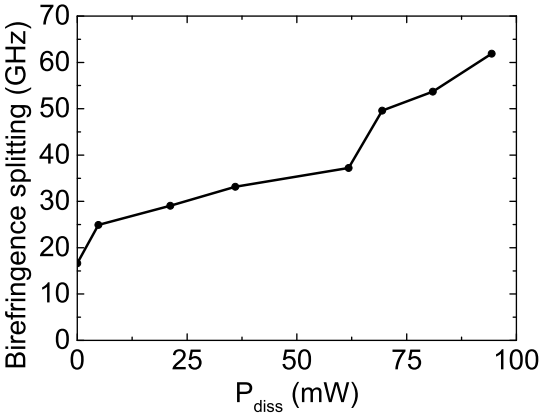

Fig. 4: Birefringence splitting of the VCSEL versus dissipated power of the integrated heater.

mechanical or piezoelectric birefringence generation to obtain high polarization oscillation frequencies with fine and wide-range tuning capability.

5. Acknowledgment

The authors thank Dr. Philipp Gerlach from Philips Technologie GmbH, U-L-M Photonics for fruitful discussions about the VCSEL design. This work has been supported by the German Research Foundation (DFG) grant "Ultrafast Spin Lasers for Modulation Frequencies in the 100 GHz Range".

References

[1] R. Michalzik (Ed.), *VCSELs — Fundamentals, Technology and Applications of Vertical-Cavity Surface-Emitting Lasers*, Springer Series in Optical Sciences, vol. 166, Berlin: Springer-Verlag, 2013.

[2] P. Moser, J.A. Lott, P. Wolf, G. Larisch, H. Li, and D. Bimberg, "Error-free 46 Gbit/s operation of oxide-confined 980 nm VCSELs at 85°C", *Electron. Lett.*, vol. 50, pp. 1369–1371, 2014.

[3] D.M. Kuchta, A.V. Rylyakov, F.E. Doany, C.L. Schow, J.E. Proesel, C.W. Baks, P. Westbergh, J.S. Gustavsson, and A. Larsson, "A 71-Gb/s NRZ modulated 850-nm VCSEL-based optical link", *IEEE Photon. Technol. Lett.*, vol. 27, pp. 577–580, 2015.

[4] T. Zuo, L. Zhang, J. Zhou, Q. Zhang, E. Zhou, and G.N. Liu, "Single lane 150-Gb/s, 100-Gb/s and 70-Gb/s 4-PAM transmission over 100-m, 300-m and 500-m MMF using 25-G class 850nm VCSEL", in Proc. *Europ. Conf. on Opt. Commun., ECOC 2016*, pp. 974–976. Düsseldorf, Germany, Sep. 2016.

[5] N.C. Gerhardt, M.Y. Li, H. Jähme, H. Höpfner, T. Ackemann, and M.R. Hofmann, "Ultrafast spin-induced polarization oscillations with tunable lifetime in vertical-cavity surface-emitting lasers", *Appl. Phys. Lett.*, vol. 99, pp. 151107-1–3, 2011.

[6] H. Höpfner, M. Lindemann, N.C. Gerhardt, and M.R. Hofmann, "Controlled switching of ultrafast circular polarization oscillations in spin-polarized vertical-cavity surface-emitting lasers", *Appl. Phys. Lett.*, vol. 104, pp. 022409-1–4, 2014.

[7] K. Panajotov, B. Nagler, G. Verschaffelt, A. Georgievski, H. Thienpont, J. Danckaert, and I. Veretennicoff, "Impact of in-plane anisotropic strain on the polarization behavior of vertical-cavity surface-emitting lasers", *Appl. Phys. Lett.*, vol. 77, pp. 1590–1592, 2000.

[8] M. Lindemann, T. Pusch, R. Michalzik, N.C. Gerhardt, and M.R. Hofmann, "Frequency tuning of polarization oscillations: toward high-speed spin-lasers", *Appl. Phys. Lett.*, vol. 108, pp. 042404-1–4, 2016.

[9] T. Pusch, M. Lindemann, N.C. Gerhardt, M.R. Hofmann, and R. Michalzik, "Vertical-cavity surface-emitting lasers with birefringence splitting above 250 GHz", *Electron. Lett.*, vol. 51, pp. 1600–1602, 2015.

[10] A.K. Jansen van Doorn, M.P. van Exter, and J.P. Woerdman, "Elasto-optic anisotropy and polarization orientation of vertical-cavity surface-emitting semiconductor lasers", *Appl. Phys. Lett.*, vol. 69, pp. 1041–1043, 1996.

[11] A.K. Jansen van Doorn, M.P. van Exter, and J.P. Woerdman, "Tailoring the birefringence in a vertical-cavity semiconductor laser", *Appl. Phys. Lett.*, vol. 69, pp. 3635–3637, 1996.

[12] M. Daubenschüz and R. Michalzik, "Parameter extraction from temperature-dependent light–current–voltage data of vertical-cavity surface-emitting lasers", in *Semiconductor Lasers and Laser Dynamics VII*, K.P. Panajotov, M. Sciamanna, A.A. Valle, R. Michalzik (Eds.), Proc. SPIE 9892, pp. 98920R-1–8, 2016.